Short Communication

Electrochemical Surface-enhanced Raman Spectroscopy for Structure Analysis of 1, 4-benzenedithiol Assembled on Gold Nanoparticles

Zhixuan Lu[*]*, Yajun Huang, and Maofeng Cao*

Department of Chemistry, College of Chemistry and Chemical Engineering, Xiamen University, Xiamen 361005, China
[*]E-mail: zhixuanlu1@gmail.com

1, 4-benzenedithiol (BDT), is a very important Raman probe molecule in the study of surface-enhanced Raman spectroscopy (SERS) because of containing benzene ring structure with large Raman differential scattering cross section and sulfhydryl group to adsorb on gold or silver nanostructures. However, there were significant differences in SERS spectra reported in different literatures, which caused interference for precise chemical measurement by using SERS spectra of BDT molecules. Here, electrochemical SERS (EC-SERS) was used to successfully analyze the spectral characteristics of BDT spontaneously forming dimers with disulfide bonds. The results showed that when the reductant $NaBH_4$ was used to pretreat BDT solution, the SERS spectra of BDT showed the characteristics of BDT monomer, similar to the spectrum of BDT assembled on gold nanoparticles (Au NPs) at negative potential. When the oxidizer H_2O_2 was used to pretreat BDT solution, the SERS spectrum of BDT showed the characteristics of BDT dimer, similar to the spectrum of BDT assembled on Au NPs at open circuit potential. This study revealed the intrinsic SERS spectrum of BDT, which is of great significance for quantitative analysis of BDT as Raman probe molecule.

1. INTRODUCTION

As a surface spectroscopy technique with chemical fingerprint information, conventional Raman spectroscopy has important applications in the study of pure sample materials [1]. However, the weak Raman scattering effect leads to the low detection sensitivity of Raman spectroscopy, which restricts the wider application of conventional Raman spectroscopy [2]. The discovery of surface-enhanced Raman spectroscopy (SERS) with as low as single molecule sensitivity solved the problem of low sensitivity of

conventional Raman spectroscopy detection [2, 3]. SERS enhancement results from surface plasmon resonance (SPR) effect of noble metal nanostructures [4]. Noteworthy, SERS effect only occurs within the range of a few nanometers on the surface of noble metal nanostructure [2]. Some target molecules are not successfully anchored within this range due to the weak interaction between target molecules and noble metal nanostructure [5]. In addition, the nature of SERS signal of some target molecules is also weak, and it is easy to be submerged by other irrelevant molecules [6].

Indirect SERS analysis method mainly uses Raman probe molecules with high SERS signal to reflect the physical and chemical properties of the studied object indirectly, which has been widely used in qualitative and quantitative detection of molecules of such targets [6]. 1, 4-benzenedithiol (BDT), is a very common Raman probe molecule in the study of SERS because of containing benzene ring structure with large Raman differential scattering cross section and sulfhydryl group to adsorb on noble metal nanostructure. By using Raman spectroscopy of BDT, the physical and chemical properties of different gold nanostructures have been performed by Kiguchi and co-workers [7]. Wan et al. realized the quantitative detection of cancer marker prostate specific antigen by using SERS spectra of BDT as internal standard [8]. By using SERS spectra of BDT, precise cell imaging was realized by Ye and co-workers [9]. However, it is worth noting that there are great differences in SERS spectra of BDT reported in literatures, which interferes with chemical analysis using SERS signals of BDT. Therefore, revealing intrinsic SERS spectrum of BDT is of great significance for realizing accurate chemical measurement. EC-SERS is able to obtain the properties of Raman probe molecules on the electrode surface under electrochemical regulation [10]. Herein, we studied the EC-SERS spectra of BDT molecule assembled on gold nanoparticles (Au NPs), explored the SERS spectra of BDT under oxidizer and reductant conditions, and successfully revealed the intrinsic SERS spectrum of BDT.

2. EXPERIMENT

2.1. Reagents and instruments

1, 4-phenyl-dimercaptan ($C_6H_6S_2$, BDT), hydroxylamine hydrochloride ($NH_2OH \cdot HCl$), chlorauric acid ($HAuCl_4$), trisodium citrate ($C_6H_5Na_3O_7 \cdot 2H_2O$) and sodium perchlorate ($NaClO_4$) were purchased from were acquired from Sigma-Aldrich (St. Louis, MO). Glassy carbon (GC) electrode with a diameter of 2 mm, a platinum wire and a Ag/AgCl electrode were acquired from Incole Union Technology Co., Ltd. (Tianjin, China). The instruments used in this paper include electrochemical workstation CHI660e (CH Instruments, Shanghai, China), field emission scanning electron microscope Hitachi S-4800 (Hitachi Japan, Ltd.), Ultraviolet visible spectrometer UV-2450 (Shimadzu Corporation, Japan) and Raman spectrometer WITec Alpha 300 R (WITec, Germany). Millipore ultrapure water (18 MΩ) was used throughout the experiments.

2.2. Preparation of AuNPs

The AuNPs were prepared by seed growth method, including the following two steps: seed synthesis and seed growth [11]. Seed synthesis: added a 125 ml 254 µM chloroauric acid aqueous

solution into a single mouth flask, heated single mouth flask until it continues to boil, and when the condensate pipe returned for about 1 second and 1 drop, stirred the solution violently to form a vortex. Quickly added 12.5 ml of 40 mM sodium citrate aqueous solution, then continue heating for 12 minutes, removed the heater, stirred for 30 minutes, and cooled it to room temperature. Seed growth: took 270 ml of ultrapure water and 30 ml of the above seed stock solution, mixed them evenly, added 3 ml of 0.2 M hydroxylamine hydrochloride aqueous solution, stirred the mix solution vigorously at room temperature for about 3 minutes, then added 2.5 ml of 25.4 mm chloroauric acid aqueous solution, and the dropping process was completed within 1 minute. Finally, the 50 nm Au NPs sol was prepared.

2.3. Preparation of SERS sample

Took 2 ml of the prepared Au NPs sol, centrifuged it at the speed of 8000 rpm/min and washed it with ultrapure water for three times. Added the concentrated liquid drops of the centrifuged Au NPs onto the polished glassy carbon electrode, and then placed the GC electrode in a vacuum drying oven for vacuum drying. The dried GC electrode was immersed in 1 mM BDT ethanol solution for 4 h, and then the sample was thoroughly washed with a large amount of ethanol and ultrapure water and dried in a vacuum dryer. The BDT modified Au NPs samples were obtained.

2.4. Measurement of Raman spectra

Measurement of the conventional Raman spectra of BDT powder. Placed an appropriate amount of BDT powder on the glass slide, covered the cover fragment and then compacted it. The white light system of WITec alpha 300 R Raman instrument was used to focus the sample, and the white light focus was controlled between the cover glass and the slide. Adjusted the experimental parameters such as laser power, exposure time and accumulation times, so that the measured Raman spectra had excellent signal-to-noise ratio, and at least three times of Raman spectra were measured continuously.

Measurement of the EC-SERS of BDT adsorbed on Au NPs. GC electrode assembled with Au NPs modified by BDT was used as working electrode, platinum wire and Ag/AgCl electrode were used as counter electrode and reference electrode respectively. The electrolyte was 0.1 M $NaClO_4$ aqueous solution. CHI660e electrochemical workstation was used for cyclic voltammetry scanning and potential control in the experiment of EC-SERS. The Cyclic voltammetry measurement were performed from -0.9 to 0.1 V in 0.1 M $KClO_4$ at a scanning rate of 10 mV/s. Raman measurement was performed when the potential was applied for 120s. Raman signal excitation laser was 633 nm, and the excitation laser was focused on the Au NPs on GC through an objective lens with a magnification of 50 and a numerical aperture of 0.55. Raman signals were collected into the signal collection optical path system through the same objective lens, and the grating used to collect Raman signals was 600 g/mm.

3. RESULTS AND DISCUSSION

3.1. Experimental design and basic characterization
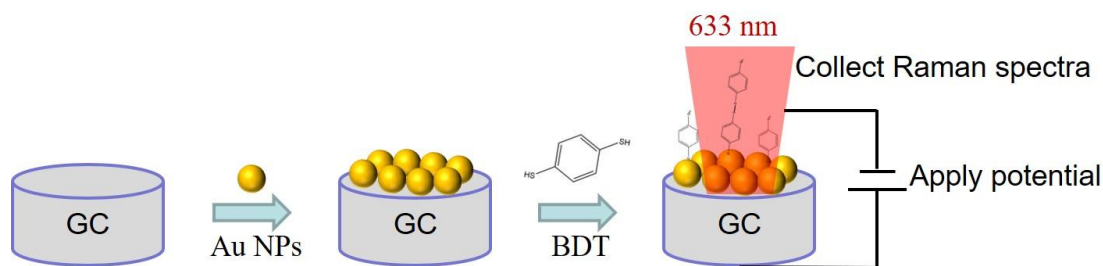
Figure 1. Schematic diagram of research strategy for studying the EC-SERS of BDT. First, Au NPs were assembled on the GC electrode, then BDT molecules were adsorbed on Au NPs, and finally the interface structure of BDT was studied by *in-situ* electrochemical Raman spectroscopy.

BDT molecule is a benzene ring structure with sulfhydryl groups at both ends. Sulfur atom in the sulfhydryl group is an asymmetric sp^3 hybrid, resulting in weak SH bond energy and easy oxidation to form S-S bond [12]. We speculate that the different SERS spectra of BDT reported in literatures may be due to the oxidation of BDT in air. In order to reveal the intrinsic SERS spectrum of BDT molecules, as shown in Figure 1, we designed the EC-SERS research strategy of BDT molecules. Firstly, Au NPs were assembled on GC electrode, and then BDT molecules were modified by immersion on Au NPs. Finally, Raman spectra of BDT under potential control were measurement. Electrochemistry can precisely control the state of molecules on the electrode surface, and SERS can obtain the chemical fingerprint information of molecules on the electrode surface. If the differences in SERS spectra of BDT reported in literature came from the oxidation of BDT molecules to form dimers, then the dissociation of dimers could be promoted by controlling electrode surface potential, so as to truly obtain intrinsic SERS spectrum of BDT, providing experimental basis for the study of BDT as Raman probe molecules.

As shown in Figure 2A, we prepared Au NPs with uniform size distribution and a diameter of approximately 50 nm. The extinction spectrum of Au NPs sol was measured by UV-Vis spectrophotometer. The SPR wavelength of Au NPs sol was about 528 nm (Figure 2B). In the sol state, it was monodisperse, mainly showing the SPR characteristics of a single Au NPs. When the Au NPs were assembled on the GC electrode, the Au NPs were in the aggregate state, there was coupling between the Au NPs, and the SPR wavelength was the real SPR wavelength position of the SERS substrate. The reflection spectrum of Au NPs assembled on the GC electrode were measured using the reflection mode of the WITec Alpha 300 R (Figure 2B). When Au NPs were assembled on the GC electrode, the SPR wavelength of Au NPs was about
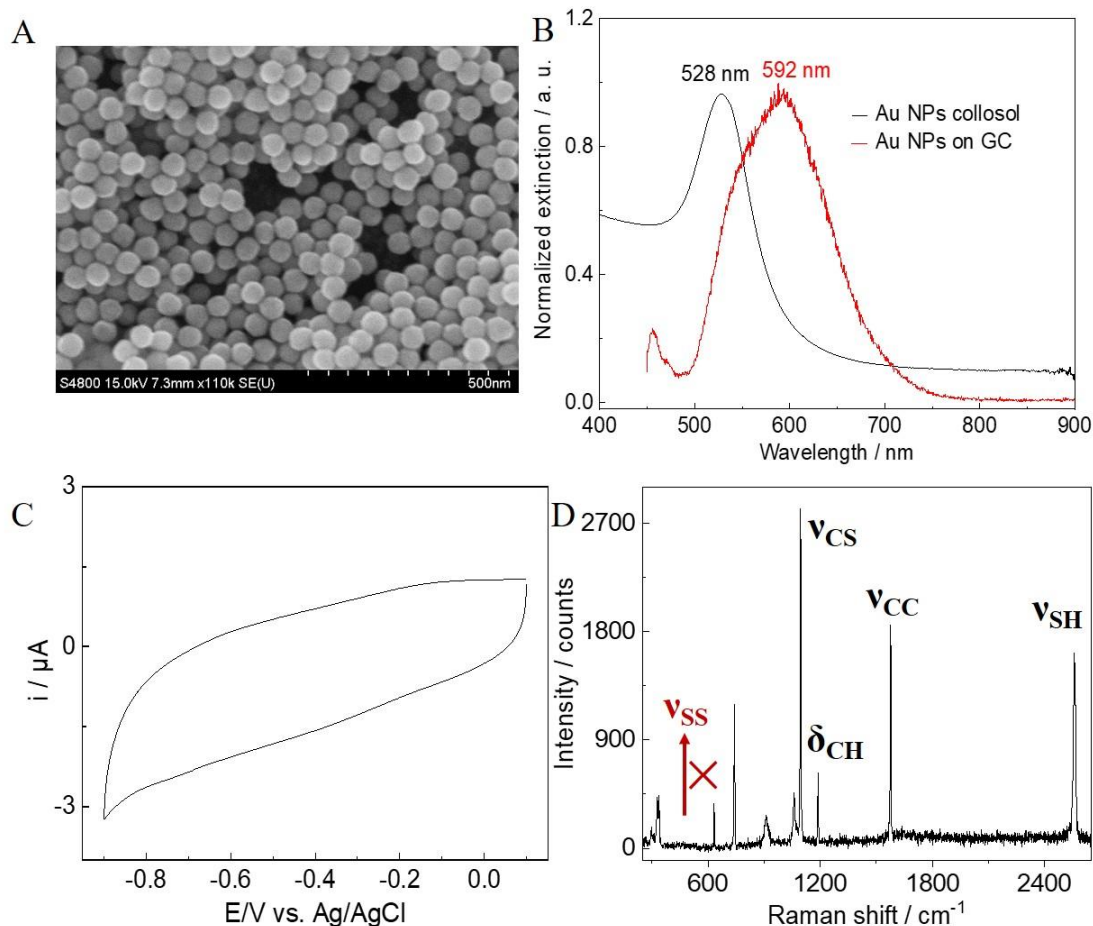
Figure 2. (A) The SEM image of Au NPs. (B) Extinction spectrum of Au NPs collosol (black) and reflection spectrum of Au NPs assembled on GC electrodes. (C) Cyclic voltammogram of BDT modified Au NPs on GC electrode acquired in 0.1 M KClO$_4$ from −0.9 to 0.1 V at a scanning rate of 10 mV/s. (D) Raman spectrum of BDT solid powder. The Raman spectrum was collected with an exposure time of 30 s and a laser power of 3 mW at 633 nm wavelength.

592 nm, which was significantly blue-shift compared with the SPR wavelength of Au NPs in the sol state. Considering that the Raman excitation laser used was 633 nm, this blue-shift made the SPR of SERS substrate closer to 633 nm, which was conducive to the enhancement of SERS signal due to the resonance effect between the laser and the SPR of Au NPs substrate [13].

Before the EC-SERS experiment, it is helpful to understand the basic electrochemical properties of BDT molecule and the conventional Raman spectrum information to analyze the EC-SERS experimental results. As shown in Figure 2C, the

cyclic voltammetric curve of BDT modified Au NPs showed that there was no obvious redox peak in the cyclic voltammetric curve within the electrochemical window of 0.1 V to -0.9 V, indicating that the BDT molecules assembled on Au NPs in this electrochemical range were macroscopically free of potential influence. However, BDT modified Au NPs showed a certain ability to activate hydrogen. The average information of the whole electrode surface was obtained by electrochemistry, but the
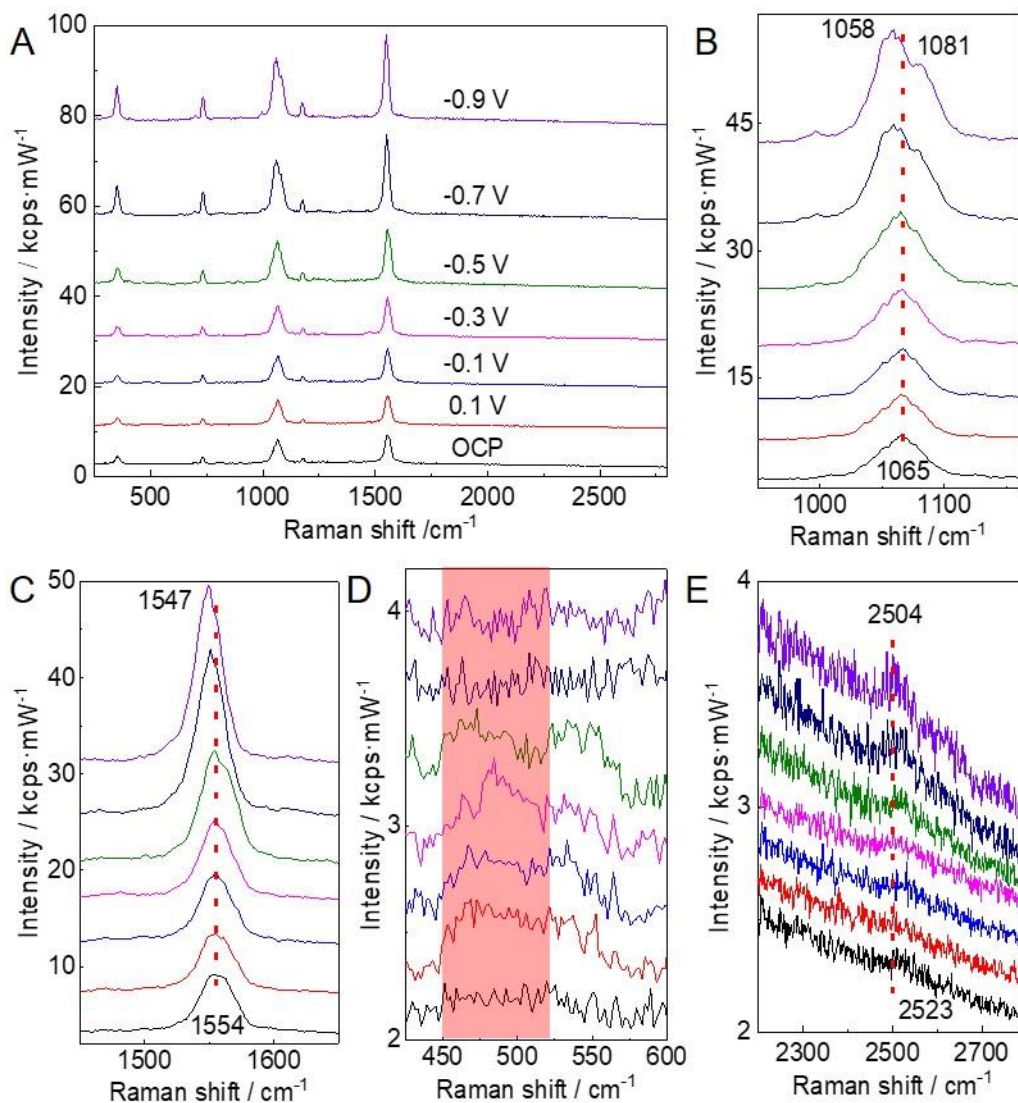
Figure 3. (A) EC-SERS of BDT modified Au NPs on GC electrode. Enlarged view of different areas for the peaks of CS (B), CC (C), SS (D) and SH (E) bond in Figure 4A. The Raman spectra were collected with a laser power of 1 mW at 633 nm wavelength.

microstructure change of BDT could not be obtained from electrochemistry experiments. Raman spectroscopy can provide molecular fingerprint information, which makes up for the lack of electrochemical experiments. Figure 2D shows the conventional Raman spectrum of BDT solid powder. It could be seen from the figure that there were several characteristic peaks in the Raman spectrum of BDT molecule, such as CS, CH, SH and CC bond on benzene ring [14]. It was worth noting that the obvious SH bond could be detected in the BDT solid powder, but the SS bond could not be detected, indicating that BDT did not oxidize into dimer in the solid powder.

3.2. EC-SERS spectra of BDT

Figure 3A shows the SERS spectra of BDT molecule at different potentials. It can be seen that with the negative shift of potential, the SERS signal of BDT as a whole gradually increased. Due to the

negative potential shift, the electrons on the electrode and the electrons on the benzene ring of BDT had a repulsive effect [10]. The structure of BDT molecules adsorption on the Au NPs would slowly change from tilt to upright. The in-plane vibration mode of chemical bonds in BDT molecules was perpendicular to the photoelectric field of excitation by laser, thus enhancing the SERS signal of BDT molecules [15].

In order to more clearly show the changes in the EC-SERS spectra of BDT molecules, we amplified the CS, CC, SS and SH bond regions, as shown in Figure 3B, C, D and E. As can be seen from the Figure 3, the Raman peak of CS bond splitted from a single 1065 cm^{-1} into two peaks 1058 cm^{-1} and 1081 cm^{-1} with the negative potential shift; the Raman peak of CC bond on benzene ring had obvious red shift at potential -0.7 V and -0.9 V; the Raman peak of SS bond was weak under the open potential, with the negative shift of potential, the Raman signal first increased, then weakened, and especially at -0.7V and -0.9V, the intensity almost decreased to zero. The Raman peak of SH bond increased with the negative shift of potential and was accompanied by red-shift. The existence of SS bond indicated that the BDT molecules modified on the surface of Au NPs had dimers. The Raman signal of SS bond itself was weak, so it can hardly be detected at the open circuit potential. However, a certain negative potential changed the adsorption configuration of BDT molecule on Au NPs and enhanced the Raman signal of SS bond. When the potential was more negative, the Raman signal intensity of SS bond decreased to zero, which indicated that the applied negative potential interrupted the SS bond. Under negative potential, the water on the electrode surface would be activated to form a reductive adsorbed hydrogen atom. The adsorbed hydrogen atom interacted with the SS bond to break the SS bond. The Raman peaks of CC bond and SH bond on benzene ring were significantly red-shift with the negative shift of potential to -0.7 V and 0.9 V. There were two symmetrical CS bonds in the BDT molecule of the monomer. When one end was modified on Au NPs, the dielectric environment of the two CS bonds was different. The Raman spectra show that the Raman frequencies of the two different CS bonds was 1058 cm^{-1} and 1081 cm^{-1}, which further proved that there was a transition from dimer to monomer in BDT. Specifically, X-ray photoelectron spectroscopy of BDT molecules self-assemble on Au film and a BDT single-molecule junction with a combined mechanically controllable break junction measurements have shown that there are dimeric BDT on the gold material modified by BDT molecule, further certifying our experimental results [16, 17]. However, compared with these two methods, our method is simpler and realizes dynamic in-situ monitoring. Therefore, based on the *in-situ* EC-SERS results of BDT molecules, we speculate that there were two molecular structures, monomer and dimer, in the BDT solution environment, and these two structures could be separated by potential regulation.

3.3. Experimental verification of BDT monomer and dimer

EC-SERS experiments showed that there were two types of BDT molecules
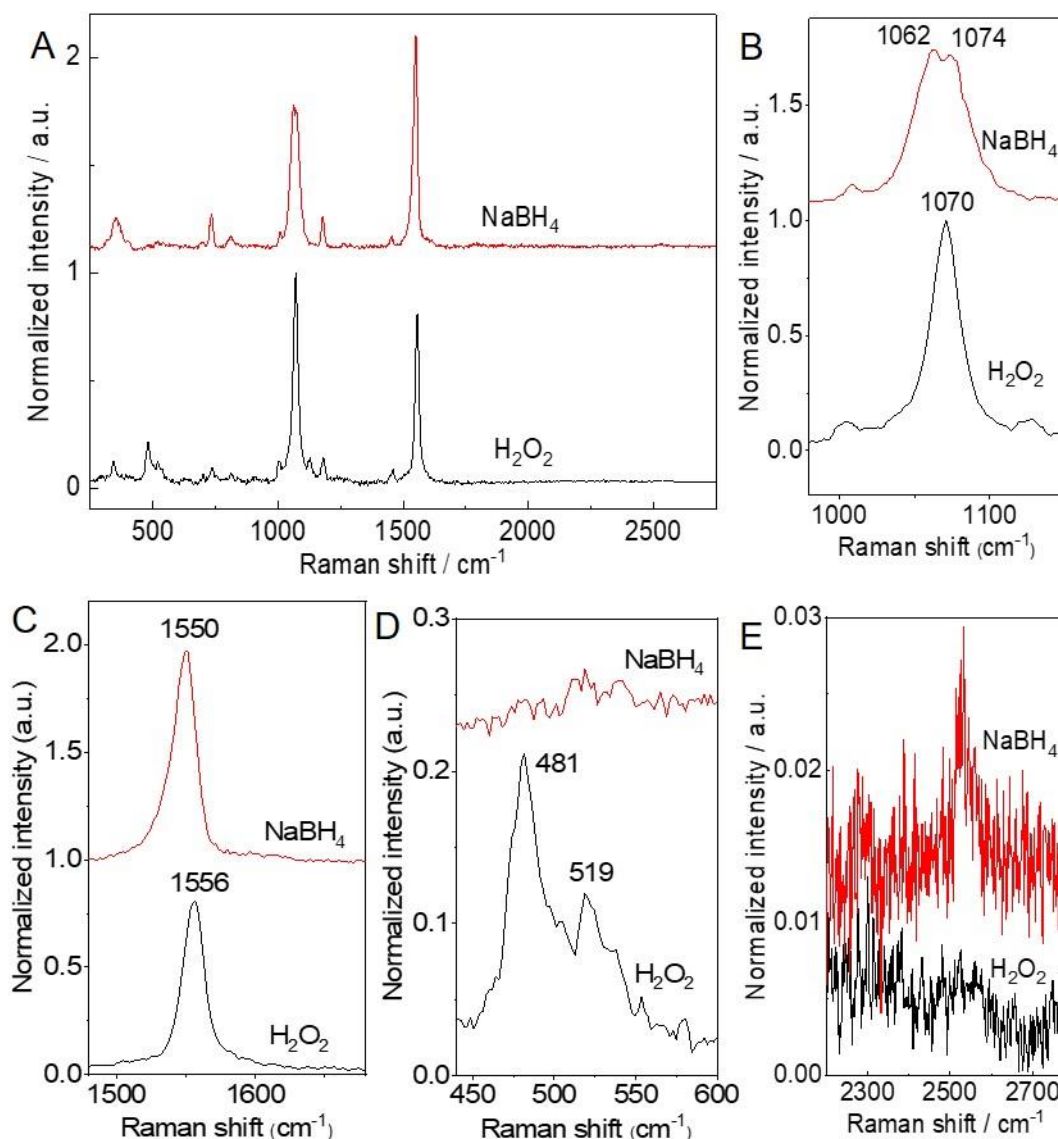
Figure 4. (A) The SERS spectra of BDT solution modified on Au NPs after treatment with $NaBH_4$ (red) and H_2O_2 (black). Enlarged view of different areas for the peaks of CS (B), CC (C), SS (D) and SH (E) bond in Figure 4A. The Raman spectra were collected with a laser power of 1 mW at 633 nm wavelength.

modified on Au NPs: monomer and dimer. BDT dimerization is actually an oxidation process, and the electrochemical negative potential controlled dimerization dissociation into monomers is actually a reduction process. If we can control the original BDT molecule to be monomer or dimer, we can obtain the real Raman spectrum information of BDT molecule. Based on this consideration, we added appropriate amounts of $NaBH_4$ or H_2O_2 to the original BDT solution. $NaBH_4$ is a strong reducing agent that can reduce SS bond to SH bond, while H_2O_2 is a neutral oxidizer that can dimerize SH bond to SS bond, which have been documented in previous reports [18, 19]. Figure 4 shows the SERS spectra of BDT solution modified on Au NPs after treatment with $NaBH_4$ and H_2O_2. It could be seen from the Figure 4 that the SERS spectra of BDT after H_2O_2 treatment were similar to those at open circuit potential: there was a Raman peak at CS bond, and the Raman peaks with SS bond and SH bond were weak. While, the SERS spectra of BDT treated with $NaBH_4$ were similar to those at -0.9 V: there were

two Raman peaks at CS bond, no SS bond Raman peak and obvious SH bond Raman peak. Therefore, with the help of pretreatment of BDT molecular solution with $NaBH_4$ and H_2O_2, it was further verified that there were two molecular structures of monomer and dimer in the environment of BDT solution, which was consistent with the results obtained from EC-SERS experiment.

4. CONCLUSION

In summary, we investigated the SERS spectra of BDT molecules by *in-situ* EC-SERS. The results showed that with the negative shift of the potential, the EC-SERS signal of BDT increased gradually and showed the phenomena of Raman peak splitting of CS bond, red-shift of Raman peak of CC and SH bond, disappearance of Raman peak of SS bond, etc. Under the negative potential, the water on the electrode surface would activate to form a reductive adsorbed hydrogen atom. The adsorbed hydrogen atom interacted with the SS bond to break the SS bond, that was, BDT changed from a dimer to a monomer. In order to confirm the results of EC-SERS experiment, BDT molecular solution was pretreated with strong reductant $NaBH_4$ and oxidant H_2O_2 respectively. It was found that the SERS spectral characteristics of BDT in the presence of oxidant were consistent with those of BDT at the open circuit. At this time, it mainly existed in the form of dimerization. The SERS spectra of BDT in the presence of reductant were consistent with those of BDT at -0.9V. At this time, it mainly existed in the form of monomer. We successfully revealed the intrinsic SERS spectrum of BDT, which is of great significance for realizing accurate chemical measurement using BDT as Raman probe molecule.

References

1.   S.Y. Ding, J. Yi, J.F. Li, B. Ren, D.Y. Wu, R. Panneerselvam, ZQ. Tian, *Nat. Rev. Mater.*, 1 (2016) 1.
2.   X. Wang, S.C. Huang, S. Hu, S. Yan, B. Ren, *Nat. Rev. Phys.*, 2 (2020) 253.
3.   M. Ge, P. Li, G. Zhou, S. Chen, W. Han, F. Qin, Y. Nie, Y. Wang, M. Qin, G. Huang, S. Li, Y. Wang, L. Yang, Z. Tian, *J. Am. Chem. Soc.*, 143 (2021) 7769.
4.   A.I. Perez-Jimenez, D. Lyu, Z. Lu, G. Liu, B. Ren, *Chem. Sci.*, 11 (2020) 4563.
5.   C. Zong, M. Xu, LJ. Xu, T. Wei, X. Ma, XS. Zheng, R. Hu, B. Ren, *Chem. Rev.*, 118 (2018) 4946.
6.   C. Zong, CJ. Chen, X. Wang, P. Hu, GK. Liu, B. Ren, *Anal. Chem.*, 92 (2020) 15806.
7.   S. Suzuki, S. Kaneko, S. Fujii, S. Marques-Gonzalez, T. Nishino, M. Kiguchi, *J. Phys. Chem. C*, 120 (2016) 1038.
8.   L. Wan, R. Zheng, J. Xiang, *Vib. Spectrosc.*, 90 (2017) 56.
9.   N.G. Khlebtsov, L. Lin, BN. Khlebtsov, J. Ye, *Theranostics*, 10 (2020), 2067.
10.   D.Y. Wu, J.F. Li, B. Ren, Z.Q. Tian, *Chem. Soc. Rev.*, 37 (2008) 1025.
11.   S. Hu, BJ. Liu, J.M. Feng, C. Zong, KQ. Lin, X. Wang, DY. Wu, B. Ren, *J. Am. Chem. Soc.*, 140 (2018), 13680.

Int. J. Electrochem. Sci., 17 **(2022)** Article Number: 220970

10

12.   J. Noh, S. Jang, D. Lee, S. Shin, Y.J. Ko, E. Ito, S.W Joo, *Curr. Appl Phys.*, 7 (2007) 605.
13.   K-Q. Lin, J. Yi, S. Hu, B-J. Liu, J-Y. Liu, X. Wang, B. Ren, *J. Phys. Chem. C*, 120 (2016) 20806.
14.   S.H. Cho, H.S. Han, D.J. Jang, K. Kim, MS. Kim, *J. Phys. Chem.*, 99 (1995) 10594.
15.   I.J. Hidi, M. Jahn, K. Weber, D. Cialla-May, J. Popp, *Phys. Chem. Chem. Phys.*   , 17   (2015) 21236.
16.   D.L. Pugmire, MJ. Tarlov, RDv. Zee, *Langmuir*, 19 (2003) 3720.
17.   J. Zheng, J. Liu, Y. Zhuo, R. Li, X. Jin, Y. Yang, Z.B. Chen, J. Shi, Z Xiao, W. Hong, ZQ. Tian, *Chem. Sci.*, 9 (2018) 5033.
18.   C.C. Winterbourn, D. Metodiewa, *Free Radical Biol. Med.*, 27 (1999) 322.
19.   J.P. Tam, CR. Wu, W. Liu, J.W. Zhang, *J. Am. Chem. Soc.*, 113 (1991) 6657.